Mon. Not. R. Astron. Soc. **000**, 000–000 (2008) Printed 29 February 2008 (MN LATEX style file v2.2)

ZOBOV: a parameter-free void-finding algorithm

Mark C. Neyrinck[1]
[1]*Institute for Astronomy, University of Hawaii, Honolulu, HI 96822, USA*
email: neyrinck@ifa.hawaii.edu

29 February 2008

ABSTRACT
ZOBOV (ZOnes Bordering On Voidness) is an algorithm that finds density depressions in a set of points, without any free parameters, or assumptions about shape. It uses the Voronoi tessellation to estimate densities, which it uses to find both voids and subvoids. It also measures probabilities that each void or subvoid arises from Poisson fluctuations. This paper describes the ZOBOV algorithm, and the results from its application to the dark-matter particles in a region of the Millennium Simulation. Additionally, the paper points out an interesting high-density peak in the probability distribution of dark-matter particle densities.

Key words: large-scale structure of Universe – methods: data analysis – cosmology: theory

1 INTRODUCTION

Voids are an essential component of the cosmic web (Bond, Kofman & Pogosyan 1996) of matter in the Universe on several-Megaparsec scales. They are fascinating from an information-theoretic viewpoint, as a probable component of efficient descriptions of large-scale structure in the non-linear regime. Voids also provide useful tools for studying cosmology and galaxy formation. The way in which matter inside a void flows away from its centre holds information about cosmological parameters such as the matter density Ω_m and dark-energy density Ω_Λ (Dekel & Rees 1994; Bernardeau & van de Weygaert 1997; Fliche & Triay 2006), and about the clustering, if it exists, of dark energy (Mota, Shaw & Silk 2008). Also, measuring the evolution of void ellipticities can give constraints on the dark-energy equation of state (Lee & Park 2007). The existence of large voids has been invoked to explain the 'cold spot' on the Cosmic Microwave Background (CMB) (Rudnick, Brown & Williams 2007); anomalously low large-angle CMB anisotropies (Inoue & Silk 2006); and even the apparent accelerating expansion of the Universe (e.g. Moffat 2006; Célérier 2007; Alexander et al. 2007). Voids are also relatively pristine laboratories to study galaxy formation and evolution, containing the most isolated galaxies in the Universe. For example, Peebles (2001) has pointed out that there seem to be fewer galaxies in voids than cosmological simulations predict. Even if this is not a discrepancy with the underlying ΛCDM cosmology, it contains valuable information about galaxy formation.

Despite these useful features of voids, they are not currently in the forefront of cosmological probes. One reason for this is that there remains no standard definition of them. The Aspen-Amsterdam Void-Finder Comparison Project (Colberg et al. 2008, AAVFCP) makes an important first step in exploring differences and similarities in void definitions, but still, a consensus about how to define a void does not exist. Here I present ZOBOV (ZOnes Bordering On Voidness), a void finder whose features, I believe, are appealing enough that it represents a net contribution toward that consensus, rather than simply adding another alternative to reconcile with the others.

Many void finders define voids as spheres, or unions of a finite number of spheres or other shapes (e.g. Kauffmann & Fairall 1991; Müller et al. 2000; Hoyle & Vogeley 2002; Colberg et al. 2005). This definition has some theoretical justification, since underdense regions expanding in a homogeneous background tend to become more spherical with time (Icke 1984). Also, this definition is geometrically simple. However, the real Universe consists of many underdense regions that collide with each other and produce voids that are often more polyhedral than spherical (e.g. Icke & van de Weygaert 1987), or even more generally shaped (Shandarin et al. 2006). ZOBOV imposes no prejudice about the shape, or even topology, of a void. Some other void finders (e.g. El-Ad & Piran 1997; Aikio & Mähönen 1998; Plionis & Basilakos 2002; Shandarin et al. 2006; Hahn et al. 2007; Aragón-Calvo et al. 2007; Platen, van de Weygaert & Jones 2007) also define voids with no, or only weak, rules about their shapes.

ZOBOV aims to find voids from a set of points with as few restrictions as possible. Conceptually, a ZOBOV void is simply a density minimum with a depression around it. ZOBOV has no free parameters. However, the ambiguity in void finding, when applied to noisy data, must be placed somewhere. With no free parameters to tune, ZOBOV returns many (indeed, mostly) shallow, hardly visible voids. However, ZOBOV measures a statistical significance for each void. A physical significance criterion can also be used, requiring that a void's minimum density $\rho_{\rm min}/\bar{\rho} < 0.2$. This is a characteristic density of a void in an Einstein-de Sitter model (with only a slightly different density in ΛCDM), obtained using a top-hat spherical expansion model (Blumenthal et al. 1992; Sheth & van de Weygaert 2004). For the abstract problem of finding voids in a particle distribution, this strategy of returning all possible voids, even statistically dubious ones (as long as they are

marked as such), seems more satisfying than making an arbitrary choice of free parameters. For many applications, though, actual use of a ZOBOV void catalogue might require another arbitrary choice, about the level of significance at which to accept a void. Another philosophical difference between ZOBOV and most void finders is that ZOBOV returns subvoids along with voids.

ZOBOV is an inversion of an 'almost-parameter-free' dark-matter-halo finder, called VOBOZ. (VOronoi Bound Zones; Neyrinck, Gnedin & Hamilton 2005, NGH). The major change in ZOBOV is that it looks for density minima instead of maxima. In fact, the VOBOZ-ZOBOV algorithm is perhaps better-suited for void finding than halo finding. This is because the algorithm typically detects highly nonspherical shapes; to get roughly spherical, virialized haloes, VOBOZ trims their edges with a boundedness criterion using particle velocities. It is in this step that VOBOZ loses its pure parameter-freedom.

Perhaps the existing void finder most similar to ZOBOV is WVF (the Watershed Void Finder; Platen et al. 2007). Both use tessellation techniques to measure densities, and both use the 'watershed' concept, defining voids with analogy to catchment basins in a density field. However, WVF uses several clever techniques from the field of mathematical morphology to smooth the particle density before defining voids, while ZOBOV analyses the raw, unsmoothed data. There are other methods that use tessellation techniques to find clusters (Ramella et al. 2001; Barkhouse et al. 2006; Söchting et al. 2006; van Breukelen et al. 2006; Melnyk, Elyiv & Vavilova 2006) or voids (Gaite 2005; Aragón-Calvo et al. 2007).

First I will discuss the ZOBOV algorithm, and then I will discuss its application to dark-matter particles in a region of the Millennium simulation (Springel et al. 2005). Some of these results appear in AAVFCP, where they are also compared to the results of other void finders. Finally, I will discuss what I feel are the unique strengths and weaknesses of ZOBOV, and what could be done to improve it.

2 METHOD

The ZOBOV algorithm is the same as the first two steps of the VOBOZ (NGH) algorithm, except that it searches for density minima instead of maxima.

2.1 Particle density and adjacency measurement

The first step is the density estimation at each dark-matter particle, using what Schaap (2007) calls the Voronoi Tessellation Field Estimator (VTFE). Tessellation methods for density estimation are widely used in many fields (e.g. Brown 1965; Ord 1978; Bülow-Olsen, Sackville Hamilton & Hutchings 1983). A good reference on this topic is provided by Okabe et al. (2000); see van de Weygaert & Schaap (2008) for a review specific to large-scale structure. The VTFE (along with its dual, the DTFE) gives arguably the most local possible density estimate that has meaningful information. The Voronoi tessellation divides space into cells around each particle, with the cell around particle i defined as the region of space closer to particle i than to any other particle. The density estimate at particle i is $1/V(i)$, where $V(i)$ is the volume of the Voronoi cell around particle i. The Voronoi tessellation also gives a natural set of neighbours for each particle (the set of particles whose cells neighbour i's cell), which ZOBOV uses in the next step.

Figure 1a shows a set of particles in 2D, corresponding to galaxies in a slice of the Millennium simulation. Figure 1b depicts the Voronoi tessellation of this set of particles, with the Voronoi cells shaded according to area.

2.2 Zoning

The second step in ZOBOV is the partition of the set of particles into zones around each density minimum. This is done partly for computational speed, and partly to compress the information in the dataset. A minimum is a particle with lower density than any of its Voronoi neighbours. ZOBOV sends each particle to its lowest-density neighbour, repeating the process until it arrives at a minimum. A minimum's *zone* is the set of particles which flow downward into it, and a zone's *core* is the minimum-density particle of the zone. Figure 1c shows how ZOBOV partitions the particles in the previous panels into zones. These zones could conceivably be called voids. Because of discreteness noise, though, many zones are spurious, and others are only the central parts of what are picked out as voids by eye. Thus, it is necessary to join some zones together to form the final voids.

2.3 From zones to voids

Zones are joined as follows. Imagine a 2D density field (represented as height) in a water tank; see, for example, Fig. 1 of Platen et al. (2007). For each zone z, the water level is set to z's minimum density, and then raised gradually. Water may flow, along lines joining Voronoi neighbours, into adjacent zones, adding them to the *void* defined around the zone z. The process stops when water flows into a deeper zone (with a lower minimum than z's), or if z is the deepest void, when water floods the whole field. The final void corresponding to z is defined as the set of zones containing water just before this happens.

The minimum-density (core) particle of the original zone is also the minimum-density particle of the zone's void. Many low-significance zones fail to annex surrounding zones as they attempt to grow; a zone in this situation has a void equal to itself. The density (water level) at which water flows into a deeper zone is recorded as $\rho_l(z)$ (l stands for 'link' to a deeper zone).

Figure 1d shows the stages of growth that the deepest void in the set of particles undergoes. Successively lighter colours shade zones added when the density level reaches successively higher levels. Since this is the deepest void, its last extent encompasses the whole simulation, except for the zone with the highest-density particle separating it from other zones, in the lower-right corner of the figure. This does not mean that other voids are not detected; they are subvoids of this largest void. Still, to form voids conforming better to intuition, a further criterion could be used to halt the growth of voids containing several zones. I will come back to this issue after discussing the statistical significance of voids, which will be useful for defining their edges.

This way of defining voids can lead to surprising void topologies and shapes. For example, if a set of particles consists of a clump surrounded by a low, uniform-density background, everything but the clump will be detected as a void. Also, even a single low-density particle along a wall between two visually apparent voids might cause ZOBOV not to detect them separately, but instead to detect a single, dumbbell-shaped void. However, many (about 16) particles directly participate in each particle's density estimate. Thus, such a hole in the wall between voids would have to be a conspiracy of many particles, and would likely look like a significant

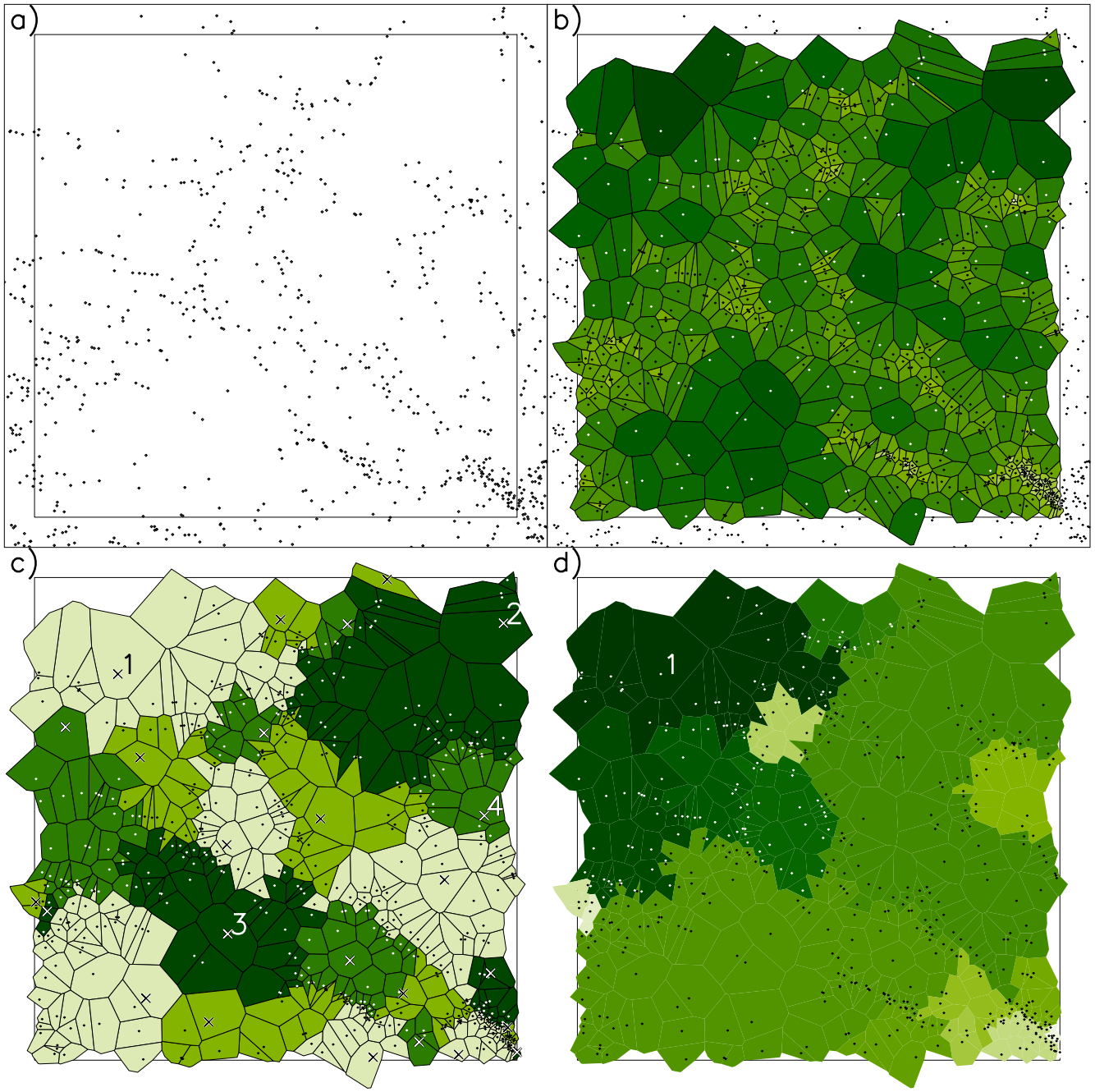

Figure 1. **(a)** Galaxies (Croton et al. 2005, down to $B = -10$) from a $40 \times 40 \times 5$ $(h^{-1}\,\mathrm{Mpc})^3$ slice of the AAVFCP region. The outer boundary is $45\,h^{-1}\,\mathrm{Mpc}$-square. The slice is the same size as the dark-matter illustration in Fig. 6, but is at an edge of the central 40-$h^{-1}\,\mathrm{Mpc}$ cube, not at the centre. It was chosen because the voids in this figure are less well-defined, and thus richer in structure. **(b)** The 2D Voronoi tessellation of galaxies in this slice, with each particle's Voronoi cell shaded according to its area. The galaxies outside the inner $(40\,h^{-1}\,\mathrm{Mpc})$ boundary are shown because they contribute to the tessellation. **(c)** Zones of galaxies. The cores (density minima) of each zone are shown with crosses, the different colours merely demarcate different zones. **(d)** The growth of void 1, the deepest void in the sample. With analogy to a water tank, the water level (density) is increased, and zones the water runs into are added to the void. Colours from dark to light indicate the stage at which the zone is added to the void. The darkest colour is the original zone, the next-darkest is the first zone or set of zones added, etc. The only zone that is never included is that with the highest-density link to another zone, in the lower-right corner. A measure of the probability that each zone-adding event leads to a void that did not arise from Poisson noise is shown in Fig. 4.

hole by eye, as well. ZOBOV operates under an implicit assumption that the discreteness noise is similar to that in a Poisson density-sampling, and ZOBOV could give surprising results if particles are carefully arranged to fool it.

2.4 Statistical significance of voids

The probability that a void v is real is judged according to its density contrast, i.e. the ratio $r(v)$ of $\rho_l(v)$, the minimum-density particle on a ridge beyond which is a deeper void, to v's minimum density, $\rho_{\min}$. This is not the only conceivable way to judge the

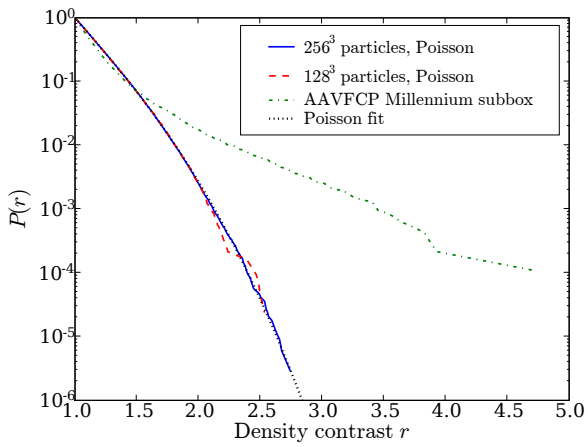

Figure 2. The cumulative probability function $P(r)$ of the ratio $r(v)$ between the lowest density of a zone and the density at which water would leak into an adjacent zone that is deeper. The solid and dashed curves show $P(r)$ for uniform-density Poisson processes using 256^3 and 128^3 particles. The curve has the same shape as the number of particles increases. The dotted curve shows the fit in Eq. (1). The dot-dashed curve shows $P(r)$ for voids in the region analysed in the Aspen-Amsterdam Void-Finder Comparison Project (AAVFCP).

significance of a void. But it is simple, and the probabilities it returns roughly align with what visual inspection would suggest.

The density contrast r is converted to a probability by comparing to a Poisson particle distribution. Several statistical properties of Voronoi diagrams applied to Poisson-sampled uniform density distributions are well-understood. For example, the distribution of Voronoi cell volumes is well-approximated by a gamma distribution (Kiang 1966), and the average number of Voronoi neighbours ($48\pi^2/35 + 2 \approx 15.54$), is even known analytically (Okabe et al. 2000). Unfortunately, the distribution of contrasts of density depressions in a Poisson Voronoi diagram is not known. It seems difficult to model analytically or from known results, since each depression has an unknown number of particles, whose estimated densities depend on each other in a complicated way. Therefore, for ZOBOV, this distribution is measured in a Monte-Carlo fashion from Poisson sampling.

Let the cumulative probability $P(r)$ be the fraction of voids in a Poisson particle distribution with density contrast greater than r. Figure 2 shows $P(r)$ as a function of r for two cubic Poisson simulations (assuming periodic boundary conditions), with 128^3 and 256^3 particles. It also shows the following fit to $P(r)$:

$$P(r) = \exp[-5.12(r-1) - 0.8(r-1)^{2.8}]. \quad (1)$$

This $P(r)$ gives an estimate of the likelihood that a void with density contrast r could arise from Poisson noise, i.e. that it is fake. Table 1 shows density contrasts corresponding to the first seven 'sigmas' (with analogy to a Gaussian distribution), calculated using this fit. The fit may be trusted to roughly $r = 3$, beyond which there is no Poisson data. In NGH, we found that the analogous significance measure for haloes seems to lose its meaning at some point between the 4- and 7-σ level anyway. That is, 7-σ haloes are not visibly more robust than 4-σ ones.

Figure 2 also shows the cumulative distribution of the density contrast r for a region of Millennium simulation, discussed in Section 3; results for this region are listed in Table 1, as well. Possibly,

σ	$P(r)$	r	Voids	Voids ($\rho_{\rm min} < 0.2$)
0	1	1	9308	5543
1	0.317	1.22	2362	1722
2	4.55×10^{-2}	1.57	525	502
3	2.70×10^{-3}	2.00	164	163
4	6.33×10^{-5}	2.45	64	64
5	5.73×10^{-7}	2.89	29	29
6	1.97×10^{-9}	3.3	13	13
7	2.56×10^{-12}	3.7	5	5

Table 1. Void abundances for various density contrasts r in a Poisson particle simulation, and in the AAVFCP region. With analogy to a Gaussian distribution, the first two columns list the levels of probability corresponding to different σ's. The third column (r) gives the density contrast with abundance $P(r)$ in a Poisson simulation, calculated using Eq. 1. The fourth column gives the number of voids exceeding density contrast r in the 40-h^{-1} Mpc AAVFCP region. The last column adds the constraint that the minimum density of the void $\rho_{\rm min} < 0.2$, in units of the mean density. The last two columns are illustrated in the top panel of Fig. 8.

a natural place to stop accepting voids as real in this data set would be where r goes below the curves' intersection, at $r \approx 1.5$. However, this occurs at about a 2-σ level, which seems quite low.

In the 256^3-particle Poisson simulation, ZOBOV detected 335025 voids; thus, the average number of particles in a zone is 50.1. This also means that one out of every 50.1 particles is a density minimum. The average number of particles in a void is greater than 50.1, though, since a void may be comprised of many zones.

The 2D version of Eq. (1) is

$$P(r) = \exp[-2.6(r-1)]. \quad (2)$$

This fit is based on a rather small set of 256^2 uniformly Poisson-distributed particles. It only extends to $P(r) \approx 10^{-3}$ (about 3 σ). This fit gives $r = 1.44$, 2.19, 3.3, 4.7, 7, 9, and 11 for significance levels of 1-7σ.

In addition to the statistical probability criterion, there is a simple physical criterion to use. The natural dark-matter density associated with a top-hat void that has undergone spherical expansion is $\rho_{\rm void} \approx 0.2$ (hereafter, densities are assumed to be in units of the mean density) at redshift 0. Because the densities of galaxies and dark matter differ in general, this criterion may be inappropriate to use for galaxies. This could be incorporated into the significance measure, for example by multiplying the probability the void is fake statistically by the probability of getting its core-particle (minimum) density $\rho_{\rm min}$ in a Poisson Voronoi diagram with density 0.2. However, in the AAVFCP sample, all ZOBOV voids statistically significant at the $\gtrsim 3\sigma$ level have core densities $\rho_{\rm min} < 0.2$ anyway (see Fig. 8). Also, the population with $\rho_{\rm min} < 0.2$ is quite distinct; there are few voids close to $\rho_{\rm min} = 0.2$. So, a simple cut-off at $\rho_{\rm min} = 0.2$ may suffice as a physical criterion, redundant if only large-significance voids are used.

2.5 Defining the edges of voids

As noted above, the deepest ZOBOV void in a set of particles will encompass all zones except the one with the highest-density ridge separating it from other zones. There are (at least) three ways to deal with this situation.

The first option is to do nothing further. The raw ZOBOV results would then consist of a large void, with several subvoids (and sub-subvoids, etc.) of varying significance levels. A zone can be-

long to multiple voids and subvoids. This option could be appealing in its simplicity, and is well-suited to the physical hierarchy that voids are thought to have in the Universe (Dubinski et al. 1993; Sheth & van de Weygaert 2004; Furlanetto & Piran 2006). However, the following two options likely produce more practically usable sets of voids.

2.5.1 *Specifying a significance level*

The second option is to excise subvoids exceeding a particular significance level (e.g., 5-σ) from parent voids. If a subvoid is removed from a void, then all zones which join the parent void in the same accretion event as that subvoid, or in subsequent ones, are also removed. This option is a natural choice if disjoint voids are desired, which is traditionally the case.

Figure 3a shows the result of this procedure, applied to the set of particles in Figure 1, using a 2-σ threshold of $r = 2.19$. According to Eq. 2, voids 1 and 2 are significant at the 4-σ level, and voids 3 and 4 are significant at the 3- and 2-σ levels. The darkest regions belong to no void over 2σ.

2.5.2 *Determining the most probable extent of voids*

The third option is to use the density contrasts of voids and subvoids to define a most-probable extent of voids. Suppose a zone z has a sequence of extents, v_i. For example, Fig. 1d shows the various possible extents for void 1 in that particle set.

At each zone-adding event, define a significance S_i. The significance of zero zone additions $S_0 \equiv P[r(z)]$, the probability of zone z's density contrast $r(z)$ arising in a Poisson particle distribution. Note that the density ratios $r(z) = \rho_l(z)/\rho_{\min}(z)$ and $r(v) = \rho_l(v)/\rho_{\min}(z)$ can differ. $\rho_l(v)$ is the lowest density among ridge particles linking z to a deeper zone (perhaps with a path through other zones), while $\rho_l(z)$ is the lowest density among ridge particles linking z to any of its neighbouring zones.

Call the void after the ith zone-adding event v_i ($v_0 \equiv z$), and call the set of zones to be added in the $(i+1)$st zone-adding event $Z_{i+1} = \{z_{i+1,j}\}$. To judge the wisdom of the $(i+1)$st addition, compare the probability that v_i and all of the zones in Z_{i+1} are individually fake to the probability that their union, $v_{i+1} = v_i + Z_{i+1}$, is fake. Given S_i, define S_{i+1} as

$$S_{i+1} = S_i \frac{P[r(v_{i+1})]}{P[r(v_i)] \prod_j P[r(z_{i+1,j})]}. \quad (3)$$

Here, $r(v_i) = \rho_l(v_i)/\rho_{\min}(z)$, where $\rho_l(v_i)$ is the the lowest density among particles on the ridge separating v_i from the set of prospective new zones Z_{i+1}. If the new zone set Z_i consists of other entire voids (i.e. sets of zones) with subvoids, only the voids, and not the subvoids, enter the product in the denominator.

For example, zone 3 in Figure 1c, and its two neighbouring zones below and to the left of it (call them $3'$ and $3''$), are separated by an insignificant (below 1-σ) density ridge, undetectable by eye in the original particle set. The probability that all three are fake (separately arose from Poisson noise) is $P[r(3)]P[r(3')]P[r(3'')] = P(1.28)P(1.11)P(1.06) = 0.30$, using Eq. (2). The probability that their union is fake is $P[r(3+3'+3'')] = P(3.57) = 0.0013$. Since the latter is rarer, the union is favoured statistically. In the S_i notation, these probabilities are normalized differently; to get the expressions in this paragraph, multiply through by the probabilities in the denominator of Eq. (3).

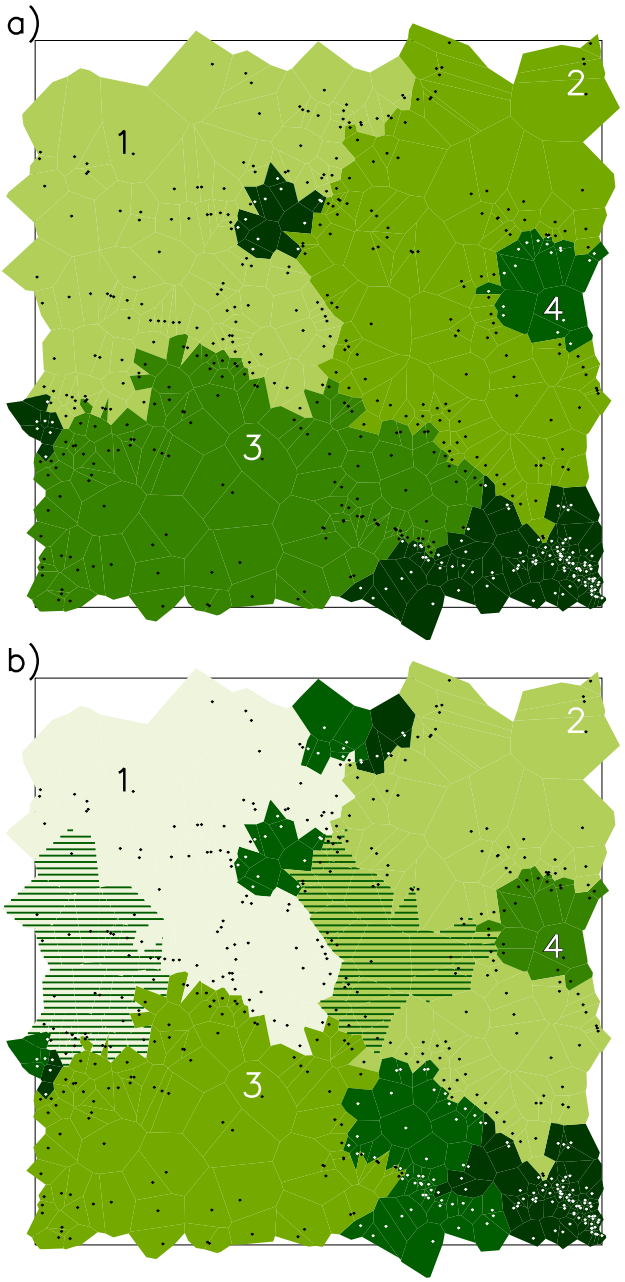

Figure 3. Two strategies for detecting the edges of highly significant voids, as applied to the particle set in Fig. 1. In **(a)**, discussed in Section 2.5.1, the user chooses a significance level at which to accept a void (here, 2-σ). Voids exceeding this threshold stop growing when they encounter another void exceeding this threshold. Particles in the darkest regions belong to no void over 2 σ. In **(b)**, discussed in Section 2.5.2, a most-probable extent is found for each void. Zones are coloured according to their significance. Zones in the deepest, 4-σ void are lightest; zones included in 3-, 2-, and 1-σ voids are coloured increasingly darkly. Particles in the darkest region belong to no void over 1 σ. The hatched regions are 1-σ subvoids.

Figure 4 shows the significances of the various possible extents for the three large voids in Fig. 1. It shows the first dip in void 3's likelihood of fakeness when the first group of zones is added, discussed in the previous paragraph. The second (and last) prospective addition, the last one before a deeper zone is encountered, gives an upturn in void 3's curve. Thus, the last addition is not favoured

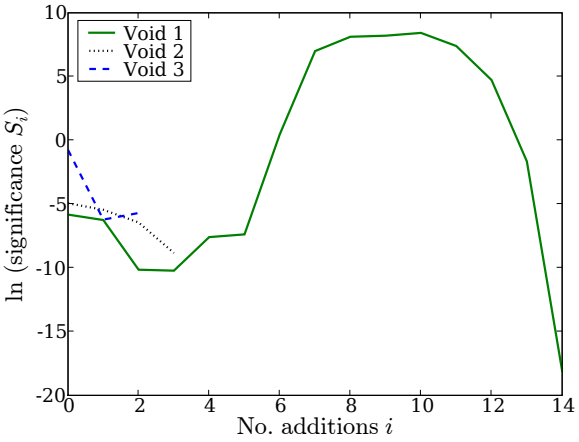

Figure 4. Significances of various extents of the three voids in Fig. 1 that encompass more than their central zone. The extents at the minima of these curves are shown in Fig. 3b, with the exception of void 1. For void 1, the extent shown in Fig. 3b has a number of additions $i = 3$, the minimum of the curve excluding the high-i ramp into high-density regions.

statistically. However, using the method of Section 2.5.1, this extra zone is included in zone 3.

Void 1, the deepest void, has the longest curve in Fig. 4. Its probability of fakeness reaches a local minimum after the third addition of zones. In accord with intuition, the curve then increases again, but then as the densest zones in the figure eventually get included, the density contrast grows sharply, making the curve plunge. ZOBOV is detecting everything except the dense points in the lower-right corner as a highly significant void. To prevent voids from growing into haloes, a density limit for links between zones may be set. For dark matter, a natural value for this limit would be $\rho_{l,\max} = 0.2$. Alternatively, one might simply accept the lowest minimum before the ramp downward at the end.

Figure 3b shows most-probable ZOBOV void extents for the 2D particle set. Zones are coloured according to their significance level. Zones in the deepest, 4-σ void (defined using three zone-addition events) are lightest; zones included in 3-, 2-, and 1-σ voids are coloured increasingly darkly. Particles in the darkest region belong to no void over 1 σ. The hatched zones are 1-σ subvoids within larger voids. All zones are actually subvoids, but most of them do not pass the 1-σ level.

2.6 Selection functions, boundaries, and holes

Observational effects complicate the application of ZOBOV to real data, e.g. from a galaxy redshift survey. This section contains some speculations about how to deal with these effects.

ZOBOV can naturally accommodate a selection function that varies with position, $\phi(\boldsymbol{x})$. All one needs to do is to divide the density of each particle/galaxy at $\boldsymbol{x}_i$ by $\phi(\boldsymbol{x}_i)$ (van de Weygaert & Schaap 2008). For void finding, densities estimated with the DTFE (defined between particles) may in general be preferable to what ZOBOV uses, the VTFE (defined at particles). However, a variable selection function is more natural to correct for using the VTFE.

ZOBOV is designed for a periodic simulation, but other boundary situations can be handled. If an isolated set of particles is analysed without any modifications, ZOBOV will still correctly determine the adjacencies of each particle. However, particles on the edge could have arbitrarily large Voronoi volumes, and thus many spurious density minima will occur on the edges. A trivial way of preventing this is to set all edge particles' densities to a value higher than any density in the interior. Another way is to add a buffer zone of particles at (for example) the mean density around the dataset. This will inhibit edge effects for densities estimated for particles a bit below the surface, as well. However, there is some ambiguity in how to make this buffer.

Holes and significantly non-convex boundaries in the data are perhaps the most difficult problem for ZOBOV. A simple way of dealing with the problem might to put particles in the holes, Poisson-sampling at the mean density inside them. The density could also be interpolated among neighbouring particles, perhaps an iterative process. Or, perhaps optimally, it could be estimated through a constrained realization (Bertschinger 1987; Hoffman & Ribak 1991; Zaroubi et al. 1995; van de Weygaert & Bertschinger 1996). With any sort of Poisson hole-filling, it would be wise to try several realizations.

Figure 5. A 5-$h^{-1}\,\mathrm{Mpc}$-wide slice through the the inner 40-$h^{-1}\,\mathrm{Mpc}$ cube analysed for the AAVFCP. This and the following figure were produced using Nick Gnedin's IFRIT software, available at `http://home.fnal.gov/~gnedin/IFRIT/`.

3 RESULTS

Here I discuss the application of ZOBOV to dark-matter particles from a cube 60-$h^{-1}\,\mathrm{Mpc}$ on a side (hereafter, the 'full cube'), taken from the Millennium simulation. Aspects of these results in the inner 40-$h^{-1}\,\mathrm{Mpc}$ cube (hereafter, the 'inner cube') can be found, with direct comparisons to other void finders, in the Aspen-Amsterdam Void-Finder Comparison Project (AAVFCP) paper. To reduce the dependence on boundary conditions, only voids with cores (minimum-density particles) in the inner cube were analysed in the AAVFCP.

ZOBOV is designed for a periodic simulation. For the non-periodic AAVFCP cube, a square lattice of particles at the mean

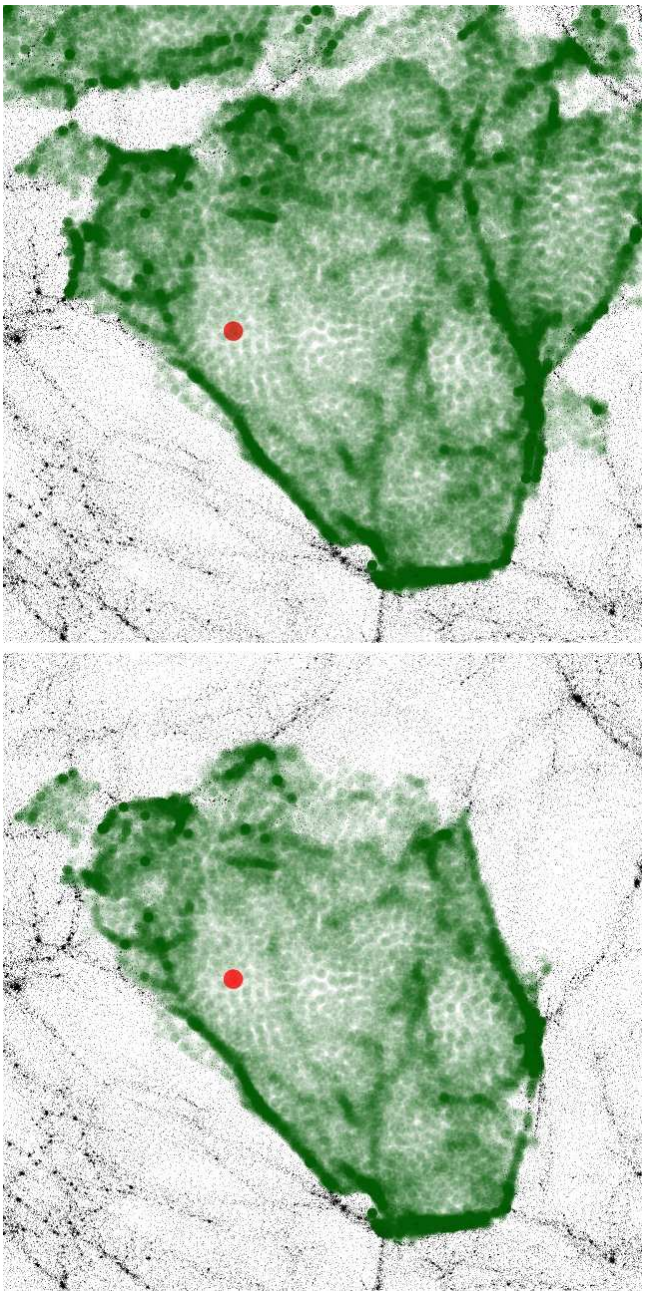

Figure 6. The largest, and most significant, void VOBOZ found the inner 40- h^{-1} Mpc AAVFCP cube. Green, diffuse particles are in the void; black particles are not. The large red dot is the core (minimum-density) particle in the void. The top panel shows the full void. The bottom panel shows the void as truncated as described in Section 2.5.1, using a significance level of 5-σ; it is the same as the most-probable extent of the void as described in Section 2.5.2, if the 'steeper fit' in Fig. 7, Eq. (4), is used.

density was added to each face of the full cube, quite far away from the inner cube (where the results are actually analysed).

ZOBOV detected a couple of orders of magnitude more voids in the AAVFCP region than almost any other void finder. This is because of the many low-significance voids, and subvoids, it detected; see Table 1, and Figure 8. The number of 5-σ voids (29) is typical of the number of voids detected by other void finders.

Figures 5 and 6 show the largest, and most significant, ZOBOV

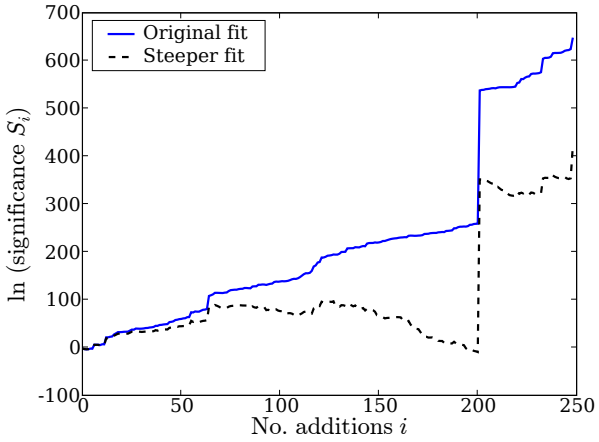

Figure 7. Significances of possible void extents for the void shown in Fig. 6. The most-probable extent (a minimum on the curve) is at $i = 2$ using the original fit to the void probability function, Eq. (1). To achieve a minimum at $i = 200$ (the extent shown in the bottom panel of Fig. 6), a steeper fit such as Eq. (4) must be used. The simulations used for Fig. 2 are too small to probe the abundance in Poisson simulations of ZOBOV voids with as high density contrast as this void.

void that has a core particle in the inner AAVFCP cube. There was actually a deeper void in the full cube, but its minimum-density particle was on the outer edge, perhaps an artefact of the boundary conditions used for the tessellation. It is this void, not the void shown in the figures, that encompasses nearly the whole volume, as the most-significant ZOBOV void typically does.

The bottom panel of Fig. 6 shows the void in the top panel, truncated as in Section 2.5.1, with a 5-σ probability threshold. It is also the most-probable extent of the void as described in Section 2.5.2, with a caveat. Figure 7 shows the extent-significance curve for this void, using two different fits of density-contrast vs. probability. The solid curve uses the original fit, Eq. (1), for $P(r)$ in Eq. (3). The minimum of this curve (showing the most-likely extent) is at $i = 2$, giving a tiny region around the central zone. There are two explanations for this discrepancy between what ZOBOV and the human eye pick out: density contrast alone is an inadequate quantifier of void significance (as judged by the human eye); or, the fit to the probability of void fakeness in Eq. (1) is inaccurate at high r.

Even using Eq. (1), there is a sharp increase in the curve at $i = 200$; the void extent at this point is shown in Fig. 6. For this to be returned as the most-probable extent, the probability of void fakeness must be dramatically reduced by a factor of e^{351} at $r = 4.5$ (the density contrast reached at $i = 200$). A steeper fit that achieves this is

$$P(r) = \exp[-5.12(r-1) - 0.8(r-1)^{4.7}], \quad (4)$$

the fit used for the dashed line. Unfortunately, the Poisson simulation used for Fig. 2 is not large enough to test the probability of such rare, high density contrasts.

3.1 Lagrangian density distribution

The top panel of Figure 8 is a scatter plot of density contrast r versus the core (minimum) density $\rho_{\rm min}$, for voids in the AAVFCP region. There are two clusters of points: one for $\rho_{\rm min} < 0.2$, about the natural density of a void in ΛCDM; and a second at high den-

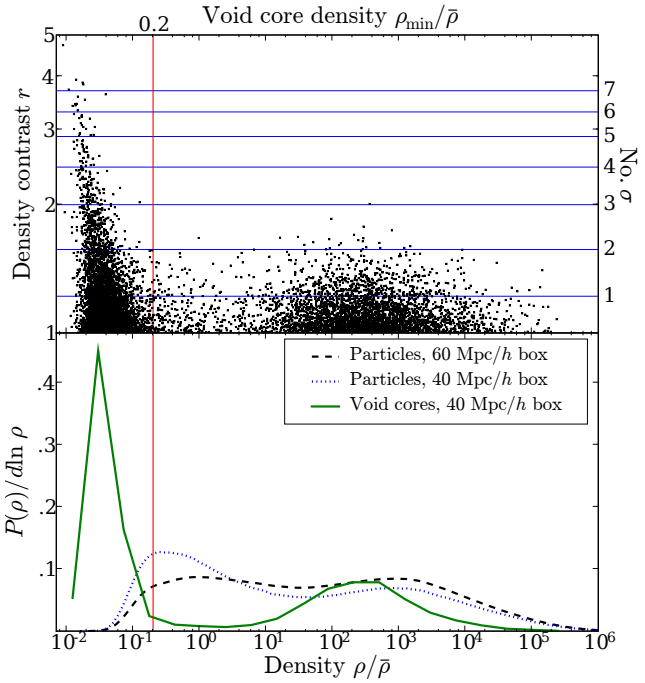

Figure 8. *Top*. For ZOBOV voids in the 40-h^{-1} Mpc AAVFCP region, a scatter plot of the minimum density $\rho_{\rm min}$, and the density contrast r (the ratio of ρ_l, the density at which a void would merge with a deeper void, and $\rho_{\rm min}$). This plot shows two populations, one that satisfies the 'physical' significance criterion, $\rho_{\rm min}/\bar{\rho} < 0.2$, and another that does not. The high-density population contains only one void above 3σ, whereas 10 would be expected from 3765 Poisson voids.
Bottom. Probability density functions (PDF's) of particle densities in the AAVFCP region. The dashed black curve shows the PDF from particles in the full 60-h^{-1} Mpc box; the dotted blue curve uses only particles in the inner 40-h^{-1} Mpc box. The inner box has fewer haloes per unit volume; this explains the lower high-density peak, and higher low-density peak, in the inner box. The solid green curve shows the PDF of void minimum-density particles. Peaks in the PDF using the full particle set (e.g. the dashed blue curve) seem to give sharper peaks in the PDF of void core-particle densities (the green curve) at slightly smaller densities.

sity, $\rho_{\rm min} \sim 10^{2.5}$. At first, the high-density group may be surprising, but all of these voids have low density contrasts. Only one of them barely passes the 3-σ level, even fewer than the expected number (10) of 3-σ objects in a sample of 3765; this is the number of voids with $\rho_{\rm min} > 0.2$. All highly significant voids above ~ 3-σ in density contrast are also physically significant, with $\rho_{\rm min} < 0.2$. This lends credence to both significance measures.

The high-density cluster in the top panel of Fig. 8 appears to be related to the high-density peak at $\rho \approx 10^{2.5}$ in the probability distribution $P(\rho)$ of particle densities, shown in the bottom panel. This peak is at approximately the fiducial density of virialization, $\rho_{\rm vir} \approx 200$, so the particles in this peak typically reside in collapsed structures. The high-density peak in $P(\rho)$ is smaller in the inner cube than in the full cube, and vice-versa for the low-density peak at $\rho \sim 1$. This makes sense, since haloes are scarce in the inner cube, most of which is occupied by a large void.

This $P(\rho)$ is approximately a Lagrangian version of the Eulerian counts in cells (CIC) statistic $P_{\rm CIC}(N, V)$ (e.g. Szapudi, Meiksin & Nichol 1996), which measures the distribution of the numbers of particles N in fixed grid cells of volume V. Roughly, $P(\rho) \propto \rho P_{\rm CIC}(N = \rho V, V)$, since, for example, each cell containing three particles will be counted once for $P_{\rm CIC}(N = 3, V)$, but thrice in $P(\rho = N/V)$. CIC measurements do not have a high-density peak, but they often have a significant high-density tail that, when multiplied by a factor of ρ (or N), may produce a peak. It would be interesting, but beyond the scope of this paper, to model this high-density peak in $P(\rho)$ using, for example, the halo model.

4 DISCUSSION

ZOBOV has a few unique, appealing features, that I believe are worth keeping in mind as cosmologists develop a standard definition of voids. These features are:

- Parameter-independence. The set of voids ZOBOV returns for a set of particles depends on no parameters, based on a simple definition of a void: a depression around a density minimum. However, the word 'depression' is also a bit vague; its definition for ZOBOV is essentially the first few paragraphs of Section 2. These implementation choices are, in a sense, parameters.
- Statistical-significance measurement for voids. Void finding is not a clear-cut business, so ZOBOV does not return a clear-cut set of results. Instead, it measures a probability that each void is real, based on how likely the void's density contrast occurs in a Poisson realization. Thus approach, I believe, is philosophically satisfying, but the raw results it returns are not necessarily straightforward to analyse. To get a definitive set of disjoint voids, one can set a significance level at which to trust that a void is real. Alternatively, ZOBOV has a mechanism to determine the most-probable extents of voids. There could be ways of analysing the raw, parameter-free ZOBOV results, as well. For example, a void probability function measurement could include all voids, but weight them by their probability of being real. ZOBOV is not the only void-finder that employs a statistical-significance test (e.g. Kauffmann & Fairall 1991).
- Hierarchical voids. Just as haloes contain subhaloes, voids contain subvoids. ZOBOV naturally accommodates this fact, detecting subvoids as well as voids. Again, a hierarchy of voids does not lend itself to straightforward analysis using traditional methods, but methods could be devised which take advantage of this hierarchical information.

There are also some areas that could benefit from further study or improvement:

- Using the (dual) Delaunay instead of the Voronoi tessellation for density estimation. The DTFE and VTFE (based on these two tessellations, respectively) give natural density estimates from a set of particles (Schaap & van de Weygaert 2000; Pelupessy, Schaap & van de Weygaert 2003; Schaap 2007). WVF (Platen et al. 2007), for instance, uses the DTFE instead of the VTFE. Both the DTFE and VTFE have no free parameters, and have infinite spatial resolution, up to machine precision. Arguably, they give the most local possible density estimates with meaningful information. The VTFE defines densities at each particle, and thus is natural for finding maxima in a set of particles. This is why we used it for the halo finder VOBOZ. However, the DTFE is a more natural choice for finding minima, since it defines densities in cells between particles. For a well-sampled density field as in an N-body simulation, the differences are likely negligible, but for sparse (e.g. galaxy) particle samples, ZOBOV should ideally use the DTFE. On the other hand, the VTFE could be preferred when faced with a vari-

able selection function, which it handles more naturally than the DTFE does.

• The definition of statistical significance for a void. ZOBOV judges the statistical significance of a void v by the contrast between the lowest density on a ridge beyond which is a deeper void, and v's minimum density. This definition is simple and easy to calculate, and the probabilities it returns compare favourably to what visual inspection suggests.

However, there are other possible significance measures. For example, the algorithm could be run several times on different Monte-Carlo realizations of the density field, formed by moving ('jittering') all particles around in some fashion corresponding to the noise in the system. If the limiting noise is from particle discreteness (which is not usually the case for actual data), a natural way to jitter the particles would be to move each particle to a random place in its initial Voronoi cell. For N-body simulations, a jitter according to a measure of the spatial resolution (e.g. the gravitational softening length) might be more appropriate. For 3D galaxy redshift surveys, the main uncertainties are probably the distances inferred from redshifts, and the handling of boundary conditions and holes. For a large data set like an N-body simulation, this Monte-Carlo approach would probably take prohibitively long, but for a more manageable dataset like a galaxy catalogue, estimating significances in this way might be tractable.

Another finding that emerged from this study is a broad, high-density peak in the logarithmically binned probability distribution of dark-matter particle densities, at $\rho \approx 10^3\bar{\rho}$, as shown in Fig. 8. It would be interesting to see whether this feature can be modelled successfully using the halo model of large-scale structure.

The code for ZOBOV, packaged with the halo-finding algorithm VOBOZ, is available at `http://ifa.hawaii.edu/~neyrinck/voboz`. The new edge-detection methods developed for ZOBOV, described in Section 2.5, make VOBOZ more attractive than previously for finding clusters in general point sets, such as galaxy catalogues.

ACKNOWLEDGMENTS

I thank István Szapudi, Erwin Platen, Sergei Shandarin, Andrew Hamilton, Nick Gnedin and Tom Bethell for helpful discussions, and the referee, Rien van de Weygaert, for insightful comments and suggestions. I also thank Volker Springel for allowing use of Millennium Simulation dark-matter coordinates, and Rien van de Weygaert and the Royal Netherlands Academy of Arts and Sciences (KNAW) for organising the wonderful December 2006 colloquium on Cosmic Voids in Amsterdam. I am grateful for support from NASA grant NNG06GE71G and NSF grant AMS04-0434413.

REFERENCES

Aikio J., Mähönen P., 1998, ApJ, 497, 534
Alexander S., Biswas T., Notari A., Vaid D., 2007, preprint (arXiv:0712.0370)
Aragón-Calvo M.A., Jones B.J.T., van de Weygaert R., van der Hulst J.M., 2007, A&A, 474, 315
Barkhouse W.A., et al., 2006, ApJ, 645, 955
Bernardeau F., van de Weygaert R., 1997, MNRAS, 290, 566
Bertschinger E., 1987, ApJ, 323, 103
Blumenthal G.R., da Costa L.N., Goldwirth D.S., Lecar M., Piran T., 1992, ApJ, 338, 234
Bond J.R., Kofman L., Pogosyan D., 1996, Nature, 380, 603
Brown G.S., 1965, New Zealand Forest Service Research Notes, 38, 1
Bülow-Olsen A., Sackville Hamilton N.R., Hutchings M.J, 1983, Oecologia, 61, 383
Célérier M.-N., 2007, New Advances in Physics 1, 29 (astro-ph/0702416)
Colberg J.M., Sheth R.K., Diaferio A, Gao L., Yoshida N., 2005, MNRAS, 360, 216
Colberg J., Pearce F., Brunino R., Foster C., Platen E., Basilakos S., Fairall A., Feldman H., Gottlöber S., Hahn O., Hoyle F., Müller V., Nelson L., Neyrinck M., Plionis M., Porciani C., Shandarin S., Vogeley M., van de Weygaert R., 2008, to be submitted to MNRAS. (AAVFCP)
Croton D.J., et al., 2005, MNRAS, 365, 11
Dekel A., Rees M.J., 1994, ApJ, 442, 1
Dubinski J., da Costa L.N., Goldwirth D.S., Lecar M., Piran T., 1993, in Chincarini G.L. et al., eds., ASPC, Vol. 51, *Observational Cosmology*, p. 188
El-Ad H., Piran T., 1997, ApJ, 491, 421
Fliche H.-H., Triay R., preprint (gr-qc/0607090)
Furlanetto S., Piran T., 2006, MNRAS, 366, 467
Gaite J., 2005, Eur. Phys. Jour. B, 47, 93
Hahn O., Porciani C., Carollo M., Dekel A., 2007, MNRAS, 375, 489
Hoffman Y., Ribak E., 1991, MNRAS, M380, L5
Hoyle F., Vogeley M., 2002, ApJ, 566, 641
Icke V., 1984, MNRAS, 206, 1
Icke V., van de Weygaert R., 1987, A&A, 184, 16
Inoue K.T., Silk J., 2006, ApJ, 648, 23
Lee J., Park D., 2007, submitted to Phys. Rev. Lett. (arXiv:0704.0881)
Kauffmann G., Fairall A.P., 1991, MNRAS, 248, 313
Kiang T., 1966, Z. Astrophys., 64, 433
Moffat J.W., 2005, JCAP 05, 001
Melnyk O.V., Elyiv A.A., Vavilova, I.B., 2006, Kinematika i Fizika Nebesnykh 22, 283
Mota D.F., Shaw D.J., Silk J., 2008, ApJ, 675, 29
Müller V., Arbabi-Bidgoli S., Einasto J.,D. Tucke D., 2000, 318, 280
Neyrinck M.C., Gnedin N.Y., Hamilton A.J.S., 2005, MNRAS, 356, 1222 (NGH)
Okabe A., Boots B., Sugihara K., Chiu S.N., 2000, *Spatial Tessellations* (New York: Wiley)
Ord J.K., 1978, Mathematical Scientist, 3, 23
Peebles P.J.E., 2001, ApJ, 557, 495
Pelupessy F.I., Schaap W.E., van de Weygaert R., 2003, A&A, 403, 389
Platen E., van de Weygaert R., Jones B.J.T, 2007, MNRAS, 380, 551
Plionis M., Basilakos S., 2002, MNRAS, 330, 399
Ramella M., Boschin W., Fadda D., Nonino, M., 2001, A&A, 368, 776
Rudnick L., Brown S., Williams L.R., 2007, ApJ, 671, 40
Schaap W.E., van de Weygaert R., 2000, A&A, 363, L29
Schaap W.E., 2007, PhD Thesis, University of Gröningen
Shandarin S., Feldman H.A., Heitmann K., Habib S., 2006, MNRAS, 376, 1629
Söcting I.K., Huber M.E., Clowes R.G., Howell S.B., 2006, MNRAS, 369, 1334
Springel V., et al., 2005, Nature, 435, 629
Sheth R.K., van de Weygaert R., 2004, MNRAS, 350, 517

Szapudi I., Meiksin A., Nichol R.C., 1996, ApJ, 473, 15
van Breukelen C., et al., 2006, MNRAS, 373, 26
van de Weygaert R., Bertschinger E., 1996, MNRAS, 281, 84
van de Weygaert R., Schaap W., 2008, in Martínez V., Saar E., Martínez-González E., Pons-Borderia M., eds, Springer-Verlag, *Data Analysis in Cosmology*. (arXiv:0708.1441)
Zaroubi S., Hoffman Y., Fisher K.B., Lahav, O., 1995, ApJ, 449, 446